A memory efficient Broyden method to simulate periodically forced processes

B.A van de Rotten and S.M. Verduyn Lunel [1]

Universiteit Leiden, Mathematical Institute, Niels Bohrweg 1, 2333 CA Leiden, The Netherlands

Abstract

The simulation of periodically forced processes in packed bed reactors leads to partial differential equations with periodic boundary conditions. These equations are naturally solved in time using numerical integration routines, but depending on the convergence properties of the system at hand, the number of cycles that needs to be computed up to a cyclic steady state is reached, can be rather large. Therefore, iterative methods to compute the cyclic steady state directly are essential. This approach might lead to severe memory constraints and, as a result, many authors use simplified approximations to simulate periodically forced processes in packed bed reactors, for example, pseudo-homogeneous one-dimensional models on a coarse grid discretization. However, simulations based on these simplified models might be inadequate or inaccurate. In this paper we propose a limited memory method, called the Broyden Rank Reduction method, and discuss some basic properties of this new singular value decomposition-based approach. The usage of the Broyden Rank Reduction method is illustrated in a concrete problem from chemical engineering.

Key words: periodically forced systems; cyclic steady states of chemical processes; quasi-Newton; method of Broyden; limited memory; singular value decomposition.

1 Introduction

Many industrial processes are operated under periodically varying, dynamic conditions. Examples of such processes are the pressure swing adsorber, the thermal swing adsorber, the reverse flow reactor [5], and the more recently developed pressure swing reactor, see the references in [13]. A common feature

[1] Corresponding author. E-mail: verduyn@math.leidenuniv.nl

of each of these processes is that the model equations are reaction-convection-diffusion equations with coefficients and boundary conditions periodic in time. After an initial transient phase the process in the reactor is determined by a limiting state that is inherently dynamic in nature, see Fig. 1. The efficient

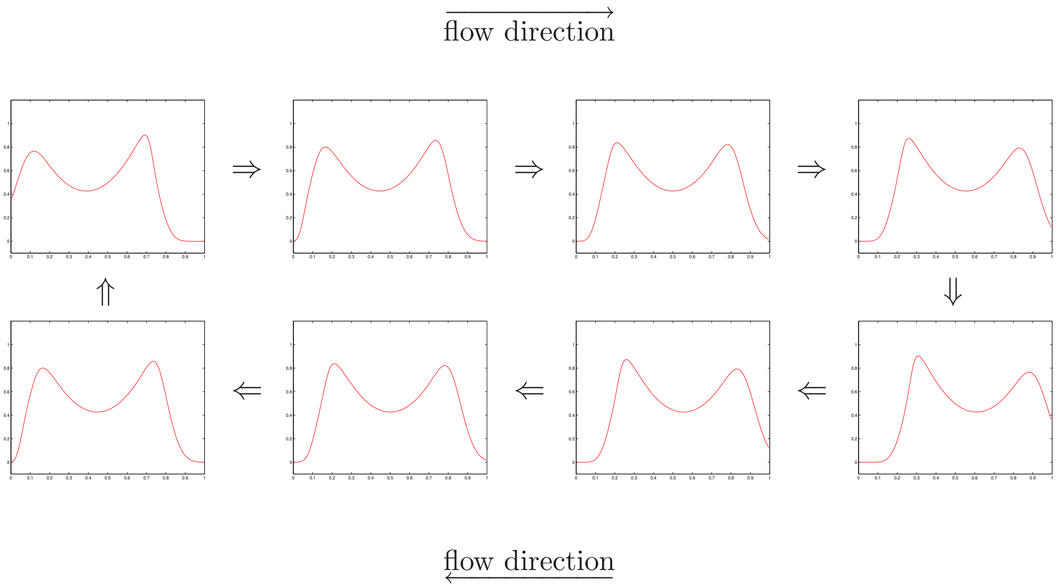

Fig. 1. An example of a cyclic steady state in a reverse flow reactor; eight snap shots of the temperature profile in axial direction.

computation of this cyclic steady state is therefore of great importance for the understanding, design and optimization of the periodically forced chemical processes.

Because of the time-dependent characteristics, a natural and obvious way to compute the cyclic steady state of a periodically forced process is to simulate its dynamic behavior. A disadvantage of this approach is that the initial transient phase may need tens of thousands of cycles, for example, in the presence of large capacity terms and slow kinetic terms [14]. In some particular cases a periodic state is never reached [5]. In optimization problems, where these calculations need to be carried out numerous times, the fact that dynamic simulations are grossly inefficient becomes a serious problem [15]. In the last decade a number of efficient iterative methods have been suggested and discussed in the chemical engineering literature. In particular, Smith and Westerberg [8] suggested the method of Broyden; and Croft and Levan [2] proposed Newton's method to compute periodic states of periodically forced processes. All simulations were restricted to pseudo-homogeneous one-dimensional models.

It is known that the radial transport of heat and matter is very important in non-isothermal packed bed reactors. In fact, a combination of a highly exothermic reaction, a large width of the reactor, and an efficient cooling of the reactor at the wall yields the existence of radial temperature gradients, see Fig. 2. Clearly, for reactors operating under these conditions the radial

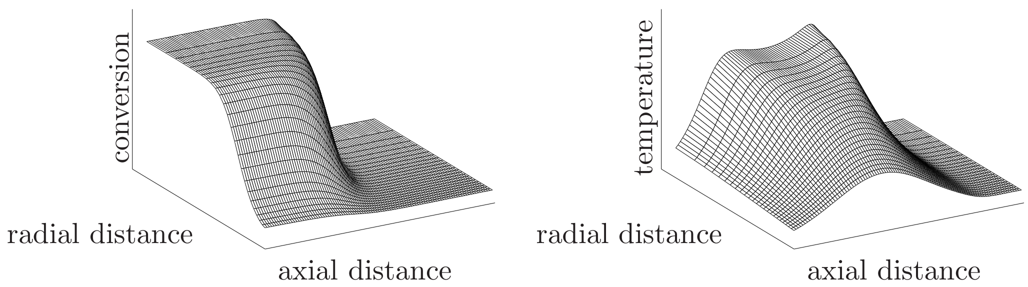

Fig. 2. Qualitative temperature and conversion distribution of the cooled reverse flow reactor using the two-dimensional model.

dimension must be taken into account explicitly [16]. This implies that for accurate computations using a fine grid discretization the number of equations of the discretized system becomes large. Consequently, it becomes practically impossible to compute the cyclic steady state using classical iterative algorithms such as the method of Broyden or Newton. The main objective of our work is to adapt the method of Broyden so that memory constraints can be avoided. This problem motivates the development of a new iterative method, called the Broyden Rank Reduction (BRR) method, which reduces the amount of memory needed to compute the periodic state of a periodically forced process significantly. To our knowledge, this is the first time that the cyclic invariant state of a periodically forced reactor is computed directly using a two-dimensional model combined with a fine grid discretization. The comparison of the BRR (p) method with other memory efficient methods like Newton-GMRES(m) as proposed by Sánchez *et al.* [6] is presented in [12].

The outline of this paper is as follows. In Section 2, we describe a two-dimensional model of a specific periodically forced process, the reverse flow reactor, including a radial dimension. The BRR method and some features of the important parameter p are discussed in Section 3. In Section 4 we describe some numerical features of the BRR(p) method, along several simulations with the system of the reverse flow reactor. In section 5 we show that the need for a more complicated two-dimensional model (including the radial dimension) exists.

2 Motivating example from chemical engineering science

As an illustrative example of a periodically forced process, we describe the operation of a reverse flow reactor, see Fig. 3. The reverse flow reactor (RFR) is a catalytic packed-bed reactor in which the flow direction is periodically reversed to trap a hot zone within the reactor. Upon entering the reactor, the cold feed gas is heated up regeneratively by the hot bed so that a reaction

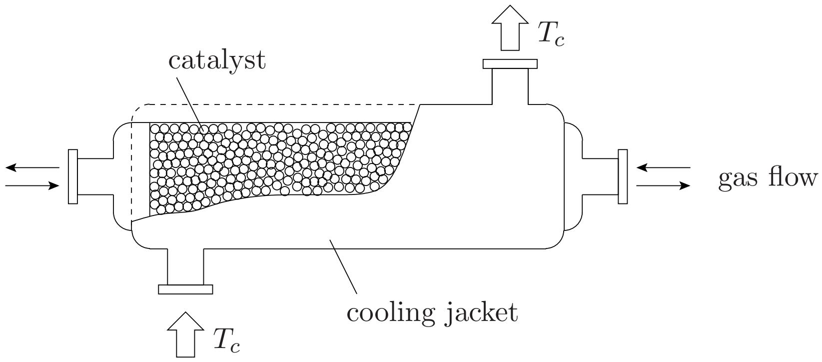

Fig. 3. Schematic drawing of the cooled reverse flow reactor.

can occur (the reaction is assumed to be exothermic). At the other end of the reactor, the hot product gas is cooled by the colder catalyst particles. So, the beginning and end of the reactor effectively work as heat exchangers. The cold feed gas purges the high-temperature (reaction) front in downstream direction. Before the hot reaction zone exits the reactor, the feed flow direction is reversed. The flow-reversal period, denoted by t_f, is usually constant and predefined. One complete cycle of the RFR consists of two flow-reverse periods, see Fig. 1. Overheating of the catalyst and hot spot formation are avoided by a limited degree of cooling.

In order to model the RFR process, we first derive the balance equations of the two-dimensional model of a general packed bed reactor starting from the one-dimensional pseudo-homogeneous model of Khinast *et al.* [5] which takes the axial heat and mass dispersion into account. The concentration and temperature depend on the axial ($0 \leq z \leq L$) and the radial ($0 \leq r \leq R$) direction, that is, $c = c(z, r, t)$ and $T = T(z, r, t)$. The second spatial dimension is incorporated by including the radial components of the diffusion terms in the component balance and the energy balance. The component balance of the two-dimensional model is given by

$$\varepsilon \frac{\partial c}{\partial t} = \varepsilon D_{\text{ax}} \frac{\partial^2 c}{\partial z^2} - u \frac{\partial c}{\partial z} - r'(c,T) + \varepsilon D_{\text{rad}} \frac{1}{r} \frac{\partial}{\partial r} \left\{ r \frac{\partial c}{\partial r} \right\}, \tag{1}$$

and the energy balance is given by

$$((\rho c_p)_s (1-\varepsilon) + (\rho c_p)_g \varepsilon) \frac{\partial T}{\partial t} = \lambda_{\text{ax}} \frac{\partial^2 T}{\partial z^2} - u(\rho c_p)_g \frac{\partial T}{\partial z} + (-\Delta H) r'(c,T) + \lambda_{\text{rad}} \frac{1}{r} \frac{\partial}{\partial r} \left\{ r \frac{\partial T}{\partial r} \right\}. \tag{2}$$

In the simulations we restrict ourselves, according to Khinast *et al.* [5], to the reaction rate given by

$$r'(c,T) = \frac{\eta k_\infty a_v k_c \exp[-E_a/R_{\text{gas}}T]}{a_v k_c + \eta k_\infty \exp[-E_a/R_{\text{gas}}T]} c. \tag{3}$$

The cooling term in the energy balance has disappeared. Instead, at the wall of the reactor we impose the boundary condition

$$\lambda_{\mathrm{rad}} \frac{\partial T}{\partial r}\bigg|_{r=R} = -U_{\mathrm{w}}(T(R) - T_c). \tag{4}$$

This boundary condition describes the heat loss to the surrounding cooling jacket. Here U_{w} denotes the heat-transfer coefficient at the reactor wall and is incorporated in the parameter Φ, the dimensionless cooling capacity, see (6). The other boundary conditions are given by

$$\begin{aligned}
-\lambda_{\mathrm{ax}} \tfrac{\partial T}{\partial z}\Big|_{z=0} &= u(\rho c_p)_g (T_0 - T(0)), & \tfrac{\partial T}{\partial z}\Big|_{z=L} &= 0,\\
-\varepsilon D_{\mathrm{ax}} \tfrac{\partial c}{\partial z}\Big|_{z=0} &= u(c_0 - c(0)), & \tfrac{\partial c}{\partial z}\Big|_{z=L} &= 0,\\
\tfrac{\partial c}{\partial r}\Big|_{r=0} &= 0, & \tfrac{\partial c}{\partial r}\Big|_{r=R} &= 0,\\
\tfrac{\partial T}{\partial r}\Big|_{r=0} &= 0.
\end{aligned} \tag{5}$$

The values of the parameters in this model are taken from [5] and summarized in Table 1.

Table 1
Parameter values for the reverse flow reactor.

$(\rho c_p)_s$	1382.0 kJ/m^{3}K	$(\rho c_p)_g$	0.6244 kJ/m^{3}K
ε	0.38	η	1
k_∞	$9.85 \cdot 10^6$ s^{-1}	k_c	0.115 m/s
a_v	1426.0 $\mathrm{m}^2_{\mathrm{surf}}/\mathrm{m}^3_{\mathrm{react}}$	E_a/R_{gas}	8328.6 K
$T_c = T_0$	323 K	ΔT_{ad}	50 K
D_{ax}	$3 \cdot 10^{-5}$ m^2/s	D_{rad}	$0.5 \cdot 10^{-5}$ m^2/s
λ_{ax}	0.01393 kW/(mK)	λ_{rad}	$1.4 \cdot 10^{-4}$ kW/(mK)
L	4.0 m	t_f	1200 s
u	1.0 m/s		

Khinast *et al.* [5] compared a one-dimensional pseudo-homogeneous or single-phase model of the reverse flow reactor and a one-dimensional heterogeneous or two-phase model. This two-phase model allowed differentiation between the solid and fluid phase. One of the objectives of Khinast *et al.* was to check if the chaotic behavior as observed using the two-phase model could also be found in the single-phase model. This turned indeed out to be the case. In order to analyze this phenomenon, they used the flow reverse time, t_f, and the dimensionless cooling capacity, given by

$$\Phi = \frac{L}{R} \cdot \frac{2U_{\mathrm{w}}}{u(\rho c_p)_g} \tag{6}$$

as bifurcation parameters.

In this work we consider the long time dynamics of the RFR for different values of the dimensionless reactor radius, denoted by R/L, and of the dimensionless cooling capacity Φ. The flow reverse time is fixed for all computations at $t_f = 1200$ s. The results are expressed in the dimensionless temperature and the conversion, respectively,

$$\theta = (T - T_0)/T_0 \qquad \text{and} \qquad x = (c_0 - c)/c_0. \tag{7}$$

Considering the dimensionless variants of (1)-(5) the heat of reaction $(-\Delta H)$ is replaced by the adiabatic temperature rise, $\Delta T_{\mathrm{ad}} = (-\Delta H c_0)/(\rho c_p)_g$.

3 A memory efficient method to simulate periodically forced processes

Periodically forced processes in plug-flow reactors can be described using a system of partial differential equations, compare the example of the reverse flow reactor discussed in Section 2. In order to simulate the dynamics of a periodically forced process numerically, we discretize the system of partial differential equations in space using a finite volumes technique with first order upwind for the convective term. The state of the reactor (temperature and concentration) at time t is denoted by a vector $x(t)$ from the n-dimensional vector space, $\mathbb{R}^n$. Here, for example, n equals two times the number of grid points used in the discretization. The resulting system of n ordinary differential equations can be written as

$$x'(t) = F(x(t), t), \tag{8}$$

where $F(\cdot, t + t_c) = F(\cdot, t)$ for $t \in \mathbb{R}$, and t_c denotes the period length.

The map $f : \mathbb{R}^n \to \mathbb{R}^n$ that assigns to an initial state at time zero, $x(0) = x_0$, the value of the solution after one cycle, $x(t_c)$, is called the Poincaré map or period map of (8). If $f(x) = (f_1(x), \ldots, f_n(x))$ and $x(t) = (x_1(t), \ldots, x_n(t))$, we have

$$f_j(x_0) = x_j(t_c), \qquad j = 1, 2, \ldots, n. \tag{9}$$

In other words, evaluating the map f is equivalent to simulating one cycle of the process (8).

From the mathematical point of view, it makes no difference whether the flow direction in the reactor is reversed or whether the reactor itself is reversed. Therefore, we do not compute the state of the RFR after one complete cycle, but instead integrate the system over one flow reverse period (t_f) and then reverse the reactor in the axial direction. The advantage of this approach is that we can use the same balance equations for both the even and odd flow reverse times. In this case, the period map f is not given by (9), but defined by

$$f_j(x_0) = x_{n-j}(t_f), \qquad j = 1, 2, \dots, n. \tag{10}$$

The state of the reactor after one complete cycle can now be obtained by applying the map f twice. A fixed point of f corresponds to a symmetric periodic state of the reactor, where the state after one flow reverse period is the mirror image of the initial state.

In order to find symmetric periodic states, we solve

$$g(x) = f(x) - x = 0. \tag{11}$$

Note that the value $f(x)$ is obtained by integrating a large system of ordinary differential equations over a period t_f. Therefore the function evaluation is a computationally expensive task and the approach that needs the fewest evaluations of f to solve (11) is the most efficient.

3.1 Iterative methods

The standard iterative algorithm to solve a system of n nonlinear equations is the method of Newton. If $x_0 \in \mathbb{R}^n$ is an initial guess in the neighborhood of a zero x^* of g, then Newton's method produces a sequence $\{x_k\}$ of approximations of x^* by the iterative procedure

$$x_{k+1} = x_k - J_g(x_k)^{-1} g(x_k), \qquad k = 0, 1, 2, \dots, \tag{12}$$

where $J_g(x)$ denotes the Jacobian of g at x. An advantage of the method of Newton is that the convergence is locally quadratic. Since it is not always possible to determine the Jacobian of g analytically, J_g is often approximated using finite differences. This results in $(n+1)$-function evaluations per iteration step, see for example [3] for details.

In 1965, Broyden [1] introduced a variant of this method that uses only one function evaluation per iteration step instead of $(n+1)$. The method of Broyden is an example of a quasi-Newton method. The key idea is to approximate the Jacobian of g by a sequence of matrices $\{B_k\}$ so that the scheme (12) can be replaced by

$$x_{k+1} = x_k - B_k^{-1} g(x_k), \qquad k = 0, 1, 2, \dots. \tag{13}$$

After every iteration step, the Broyden matrix B_k is updated by adding a specific rank-one-matrix. The updated Broyden matrix B_{k+1} is chosen such that it satisfies the equation

$$B_{k+1}s_k = y_k, \tag{14}$$

with $s_k = x_{k+1} - x_k$ and $y_k = g(x_{k+1}) - g(x_k)$. If we assume that B_{k+1} and B_k are identical on the orthogonal complement of the linear space spanned by s_k, condition (14) results in the following update scheme for the Broyden matrix B_k,

$$B_{k+1} = B_k + (y_k - B_k s_k)\frac{s_k^T}{s_k^T s_k} = B_k + \frac{g(x_{k+1})s_k^T}{s_k^T s_k}. \tag{15}$$

Equation (14) is called the secant equation and quasi-Newton algorithms that satisfy this condition are called secant methods [3].

Remark 1 *If we choose $B_0 = -I$ as an initial guess for the Broyden matrix in* (13)*, then $x_1 = x_0 + g(x_0) = f(x_0)$, i.e., the first iteration step corresponds to iterating the map f itself. In applications, this is often a good strategy to start the simulation.*

3.2 Basics of the Broyden Rank Reduction method

Both Newton's and Broyden's method need to store an $(n \times n)$-matrix, compare (12) and (13), and for high-dimensional systems this might lead to severe memory constraints. From the early seventies serious attention has been paid to the issue of reducing the amount of storage required for iterative methods. Different techniques have been developed for solving large nonlinear problems [4,7,10]. Because the method of Broyden is often used effectively in chemical reactor engineering, it is our aim to focus on an approach that reduces the memory used by the method of Broyden. We call such algorithms *limited memory Broyden methods.*

The main new algorithm that we would like to propose here is called the Broyden Rank Reduction method (BRR). The BRR method is a singular value decomposition-based approach exploiting the fact that the Broyden matrix can be given as the sum of the initial Broyden matrix and a number of rank one updates.

Starting with an initial estimate vector x_0 and an initial estimate matrix B_0, the first Broyden matrix is given by,

$$B_1 = B_0 + c_1 d_1^T,$$

where $c_1 = g(x_1)/\|s_0\|$ and $d_1 = s_0/\|s_0\|$, see (15). If there is no need to store B_0, for example when $B_0 = -I$, then it is more efficient to store the vectors

c_1 and d_1 rather than the matrix B_1 itself. After applying the next update, the new Broyden matrix B_2 is given by

$$B_2 = B_1 + c_2 d_2^T = B_0 + Q_2,$$

where the update matrix Q_2 is given by

$$Q_2 = c_1 d_1^T + c_2 d_2^T$$

where $c_2 = g(x_2)/\|s_1\|$ and $d_2 = s_1/\|s_1\|$. Now $4n$ locations are used to store the vector pairs $\{c_1, d_1\}$ and $\{c_2, d_2\}$. In the next iteration step, we need $6n$ storage locations to store all of the vector pairs, etc. In the k^{th} iteration step the update matrix Q_k consists of k rank-one updates to the initial Broyden matrix B_0 and, therefore, has rank less or equal to k. The singular value decomposition of the update matrix Q_k reads

$$Q_k = \sigma_1 u_1 v_1^T + \ldots + \sigma_k u_k v_k^T,$$

where $\{u_1, \ldots, u_k\}$ and $\{v_1, \ldots, v_k\}$ are orthonormal sets of vectors and $\sigma_1 \geq \ldots \geq \sigma_k \geq 0$. An important result of the singular value decomposition of the update matrix Q_k is that

$$Q_k^{(l)} = \sum_{j=1}^{l} \sigma_j u_j v_j^T, \qquad l < k,$$

is the best rank-l matrix approximation to Q_k with respect to the Frobenius norm, see Strang [9].

In order to use a limited amount of memory to store the Broyden update matrix, we fix an integer p. As long as $k < p$, we perform a Broyden update step, but as k reaches the value p, we reduce memory by ignoring the rank one contribution corresponding to the smallest singular value σ_p of the update matrix Q_p. So we replace the update matrix Q_p by a modified update matrix $\widetilde{Q}_p$ given by

$$\widetilde{Q}_p = Q_p - \sigma_p u_p v_p^T = \sum_{j=1}^{p-1} \sigma_j u_j v_j^T.$$

Next we set

$$c_i := \sigma_i u_i \qquad \text{and} \qquad d_i := v_i \qquad \text{for } i = 1, \ldots p-1,$$

so that the new reduced update matrix $\widetilde{Q}_p$ has a similar representation as the previous update matrix Q_{p-1}. Since the modified update matrix $\widetilde{Q}_p$ has rank $p-1$, we have created space to store a new pair of update vectors produced by the $(p+1)^{th}$-Broyden step.

We continue this procedure; before we can add a new update, we first compute the singular value decomposition of the update matrix Q_k and then remove the rank one contribution corresponding the smallest singular value. Next we store the new pair of update vectors produced by the $(k+1)^{th}$ Broyden step. So, the update matrix in the BRR method has at most rank p, where p is an integer that can be fixed a priori depending on the characteristics of the period map at hand or the underlying system of partial differential equations.

Example 2 Consider the system (11) where the period map $f : \mathbb{R}^n \to \mathbb{R}^n$ is a small ($\varepsilon = 10^{-2}$) quadratic perturbation of two times the identity map,

$$f(x) = (2x_1 - \varepsilon x_2^2, \ldots, 2x_{n-1} - \varepsilon x_n^2, 2x_n), \tag{16}$$

where we take $n = 10^5$. We apply the BRR method for $p = 5$ to approximate the unique solution of $g(x) = f(x) - x = 0$ up to a residual of $\|g(x)\| < 10^{-12}$. The initial estimate vector is set to $x_0 = (1, \ldots, 1)$ and the initial matrix to $B_0 = -I$. After the fifth iteration the singular values of the update matrix Q_5 read

$$\sigma_1 = 2.5, \quad \sigma_2 = 1.6, \quad \sigma_3 = 2.1 \cdot 10^{-6}, \quad \sigma_4 = 1.2 \cdot 10^{-13}, \quad \sigma_5 = 0.0.$$

This supports the idea that it is not harmful to remove the fifth term of the singular value decomposition of the update matrix and store the new pair of update vectors using $c_5 := g(x_6)/\|s_5\|$ and $d_5 := s_5/\|s_5\|$. The computation shows that after 14 iterations the convergence criterion is satisfied. The rate of convergence of this process is plotted in Fig. 4, together with the rate of convergence of the BRR method for values of p ranging from 1 to 5. For

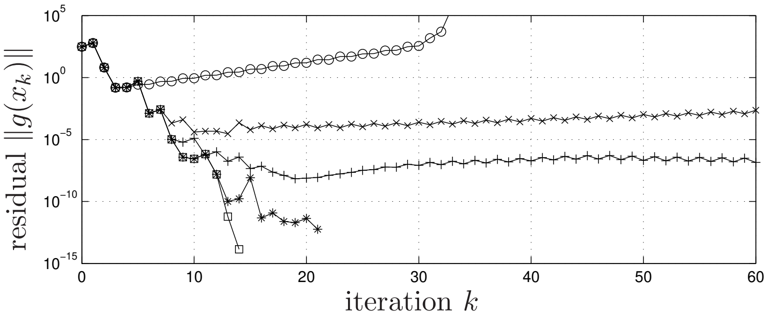

Fig. 4. The convergence rate of the Broyden Rank Reduction method when computing a fixed point of the function f given by (16). ['$\circ$'($p = 1$), '$\times$'($p = 2$), '$+$'($p = 3$), '$*$'($p = 4$), '$\Box$'($p = 5$)]

$1 \leq p \leq 3$ too much information contained in the Broyden update matrix is lost and the scheme fails to converge. For $p \geq 4$, the scheme does converge. Interestingly, for $p \geq 5$, the rate of convergence of the scheme is stable and does no longer increase for larger values of p. We call this value of p the optimal value for the BRR method. Note that with $p = 5$, the number of required storage locations for the Broyden update matrix is reduced from $n^2 = 10^{10}$ for the matrix of the original method of Broyden to $2pn = 10^6$ for the matrix of the BRR method, at no additional cost.

Since $p \ll n$, the example shows that the BRR method can reduce the amount of storage needed for the Broyden update matrix significantly. In order to investigate the dependence of p on the dimension of the system, we have repeated the simulations of Example 2 for different values of n ($n = 100$, $n = 1000$, $n = 10000$). In these simulations the choice of an optimal p is actually independent of the value of n. This robustness property of p is subject of further study and it is an interesting problem to understand which properties of the dynamical system determine an optimal value of p. We return to this problem in Section 4.

3.3 Features of the Broyden Rank Reduction method

We can represent the rank one updates to the initial Broyden matrix B_0 after the k^{th} iteration as the columns of two matrices $C_k = [c_1, \ldots, c_k]$ and $D_k = [d_1, \ldots, d_k]$. This implies the Broyden update matrix can be represented by

$$Q_k = C_k D_k^T.$$

The parameter p in the BRR method denotes the maximal rank of the Broyden update matrix Q_k. If we choose B_0 to be minus the identity ($B_0 = -I$), then we have to store at most $2pn$ elements (of the matrices C_k and D_k) in order to have the Broyden update matrix Q_k.

This representation of the Broyden update matrix has the advantage that the Sherman-Morrison-Woodbury formula (17) can be used in order to compute the inverse of the Broyden matrix [3].

Lemma 3 *Let B be a nonsingular $(n \times n)$-matrix and C, D be arbitrary $(n \times p)$-matrices with $p \leq n$. If $(I + D^T B^{-1} C)$ is nonsingular then $(B + CD^T)^{-1}$ exists and*

$$(B + CD^T)^{-1} = B^{-1} - B^{-1}C(I + D^T B^{-1} C)^{-1} D^T B^{-1}. \tag{17}$$

PROOF. The formula (17) can easily be verified by simplifying the expressions

$$(B^{-1} - B^{-1}C(I + D^T B^{-1} C)^{-1} D^T B^{-1})(B + CD^T),$$

and

$$(B + CD^T)(B^{-1} - B^{-1}C(I + D^T B^{-1} C)^{-1} D^T B^{-1}).$$

Since both expressions are equal to the identity, it follows that $B + CD^T$ is invertible and the inverse is given by (17).

The BRR method is actually a feasible method in practice. In fact, in the BRR method the k^{th} approximation, x_k, can be obtained by solving a system of linear equations of rank at most p. By choosing $B_0 = -I$, the inverse of the Broyden matrix yields

$$B_k^{-1} = (-I + C_k D_k^T)^{-1} = -I - C_k(I - D_k^T C_k)^{-1} D_k^T,$$

where $I - D_k^T C_k$ is an $(p \times p)$-matrix. Furthermore, the next lemma shows that the computation of the singular value decomposition of the Broyden update matrix Q_k can be reduced to the computation of the eigenvalues and corresponding eigenvectors of an $(p \times p)$-matrix.

Lemma 4 *Let A be an $(n \times n)$-matrix and p an integer less than or equal to n. If $A = CD^T$ with C, D arbitrary $(n \times p)$-matrices, then the n-dimensional problem of the computation of the singular values of the matrix A can be reduced to the computation of the eigenvalues of an $(p \times p)$-matrix.*

PROOF. Let the QR-decomposition of D be given by

$$D = QR$$

and let the singular value decomposition of CR^T be given by

$$CR^T = U \Sigma W^T$$

then

$$A = CD^T = C(QR)^T = CR^T Q^T = (U \Sigma W^T) Q^T = U \Sigma (QW)^T.$$

The singular values of CR^T are the square roots of the eigenvalues of the matrix $(CR^T)^T CR^T$, which is indeed an $(p \times p)$-matrix. Since that matrices Q and W are orthogonal, the product QW is orthogonal as well. This completes the proof.

Remark 5 *The rank reduction which we apply to the Broyden update matrix Q_k can also be interpreted as follows. For the method of Broyden, the action of the Broyden matrix has to be known in all n directions, in order to compute the new Broyden step s_k, compare* (13). *In the BRR method we only know the action of the Broyden matrix in at most p directions, but these p directions are produced and modified during the iterations by the Broyden process itself. This turns out to be rather effective in practice.*

The pseudo-code of the Broyden Rank Reduction method is described in Algorithm 1. Given a system of nonlinear equations (11) with $g : \mathbb{R}^n \to \mathbb{R}^n$, the algorithm for the Broyden Rank Reduction (p) method uses $2pn$ storage location instead of n^2 in order to store the Broyden matrix.

Algorithm 1 *Choose an initial estimate $x_0 \in \mathbb{R}^n$, set the parameter p, and let the $(n \times p)$-matrices $C = [c_1 \cdots c_p]$ and $D = [d_1 \cdots d_p]$ be initialized by $c_i = d_i = 0$ for $i = 1, \ldots, p$. Set $k := 0$ and repeat the following sequence of steps until $\|g(x_k)\| < \varepsilon$.*

i) Solve $(I - D^T C)t_k = -D^T g(x_k)$ for t_k and set $s_k := -g(x_k) + Ct_k$,
ii) Set $x_{k+1} := x_k + s_k$ and $y_k := g(x_{k+1}) - g(x_k)$,
iii) Compute the QR-decomposition of $D = QR$, where Q is an orthogonal $(n \times p)$-matrix and R an upper triangular $(p \times p)$-matrix,
$D := Q, \qquad C := CR^T,$
iv) Compute the singular value decomposition of $C = U\Sigma W^T$, where U, W are orthogonal $(n \times p)$-matrices and $\Sigma = diag\,(\sigma_1, \ldots, \sigma_p)$, where $\sigma_1 \geq \cdots \geq \sigma_p \geq 0$,
$C := U\Sigma, \qquad D := DW,$
v) Set $c_p := (y_k - (-I + CD^T)s_k)/\|s_k\|$ and $d_p := s_k/\|s_k\|$,
vi) $k := k + 1$.

Remark 6 *Note that we apply the reduction procedure of the Broyden update matrix Q_k before the new update is computed. This implies that the BRR method is still a secant method.*

Remark 7 *The difference in Frobenius norm between the full Broyden matrix B_k and the reduced Broyden matrix $\widetilde{B}_k = B_k - \sigma_p u_p v_p^T$ produced by the BRR method, is given by*

$$\|B_k - \widetilde{B}_k\| = \|\sigma_p u_p v_p^T\| = \sigma_p,$$

where σ_p denotes the pth singular value of the update matrix Q_k and u_p and v_p are its corresponding left and right singular vectors, respectively. In particular, as long as $k \leq p$, the BRR scheme is equal to the Broyden scheme as $\sigma_p = 0$ for $k = 1, \ldots, p - 1$.

4 Simulations of the periodic states of the reverse flow reactor

In this section we illustrate the usage of the BRR method in a concrete problem from chemical engineering. We will show that the Broyden Rank Reduction method can effectively be used to simulate the full two-dimensional model of the reverse flow reactor presented in Section 2.

A general disadvantage of iterative methods is the choice of an appropriate initial approximation of the solution as well as an appropriate initial Broyden matrix. Interestingly, the application at hand provides these initial conditions very natural. The reverse flow reactor is usually started in preheated state ($T = 2T_0$, so $\theta = 1$) where the reactor is filled with the carrier gas without a trace of the reactants ($c = 0$, so $x = 1$). This initial state of the reactor is chosen as the initial state x_0 of the Broyden process, that is $x_0 = (1, \ldots, 1)$. As we have seen before, taking the initial Broyden matrix equal to minus the identity, $B_0 = -I$, implies that the the first iteration of the Broyden process equals a dynamical simulation step. Again very natural in the context of a dynamical system.

We first discretize the system of partial differential equations (1)-(5) in space. For the finite volume discretization an equidistant grid is used with N grid points in the axial direction ($N = 100$). For the component balance equation the first order upwind discretization is used and for the energy balance equation the central discretization. In the radial direction a non-uniform grid of M grid points is chosen that becomes finer in the direction of the wall of the reactor ($M = 25$). In fact, a segment of the reactor is divided in M rings with the same volume. The state vector of the dynamical system, denoted by x, consists of the temperature and the concentration in every grid point. The dimension of the discretized system is denoted by n ($n = 2 \cdot N \cdot M = 5000$). The system of ordinary differential equations is integrated over one reverse flow period using the NAG-library routine D02NCF.

Let $f : \mathbb{R}^n \to \mathbb{R}^n$ be the period map of the RFR defined in (10) We choose the bifurcation parameters to be $R/L = 0.0025$ and $\Phi = 0.2$. To solve equation (11) the BRR method is applied for different values of p. It turns out that for the two-dimensional model it is not possible to apply Broyden's method directly, due to memory constraints. In Fig. 5 it is shown that the BRR method

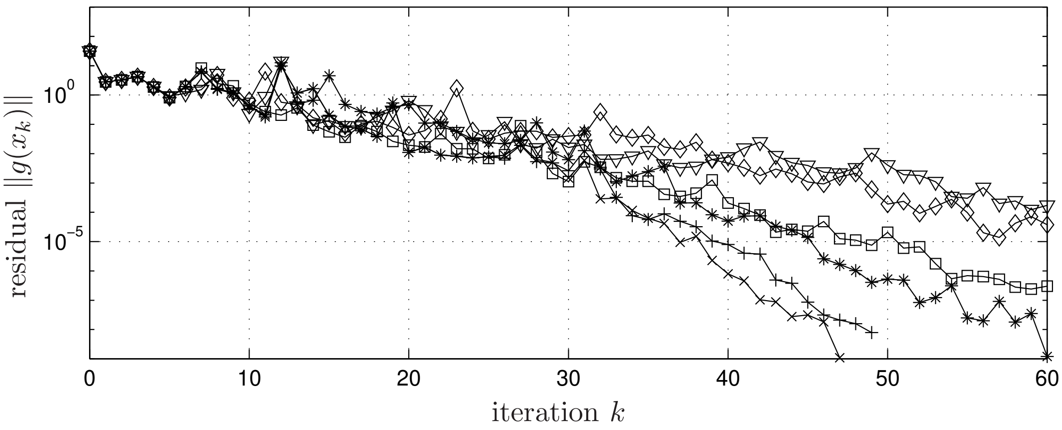

Fig. 5. The convergence rate of the BRR(p) method, applied to the period map of the reverse flow reactor, with $R/L = 0.0025$ and $\Phi = 0.2$. ['$\times$' ($p = 20$), '+' ($p = 10$), '$*$' ($p = 5$), '$\square$' ($p = 4$), '$\diamond$' ($p = 3$), '$\triangledown$' ($p = 2$)]

has a high rate of convergence for $p \geq 5$. For $2 \leq p \leq 4$ the BRR method does not converge within 60 iterations. The amount of memory needed to store the Broyden matrix can be reduced by choosing $p = 10$ instead of $p = 20$, using approximately the same number of iterations.

For the above simulation of the two-dimensional model a thin reactor is used ($R/L = 0.0025$). In this case gradients in the radial direction are absent and the two-dimensional model leads to exactly the same results as the one-dimensional pseudo-homogeneous model. If we increase the radius of the reactor ($R/L = 0.025$), then radial temperature gradients are in fact present.

4.1 Finer grid using same amount of memory

To illustrate the benefits of our limiting memory method we compare two simulations of the model with $M = 25$ and $M = 5$ grid points in the radial direction. So the dimension of the discretized problem becomes $n = 5000$ and $n = 1000$, respectively. We have applied the BRR method with different values of p to compute the periodic state of the reactor, see Table 2.

Table 2
The number of iterations needed by the BRR method to solve (11), corresponding to the two-dimensional problem of the RFR, and the number of storage locations for the Broyden matrix ($N = 100, R/L = 0.025$ and $\Phi = 0.2$).

	$M = 25$		$M = 5$	
	# iterations	# storage locations	# iterations	# storage locations
$p = 20$	48	200,000	53	40,000
$p = 10$	50	100,000	55	20,000
$p = 5$	61	50,000	65	10,000
$p = 4$	65	40,000	82	8,000
$p = 3$	80	30,000	76	6,000

Although a few more iterations are needed than in case of the thin reactor ($R/L = 0.0025$), still the same values for p can be used for both the fine and the coarse grid. Note that for every value of p the convergence for $M = 25$ is faster than for $M = 5$. Suppose, however, that at most 40,000 storage locations are available. Given this imposed memory constraint we use the largest possible value of p to obtain the highest rate of convergence. For the coarse grid p can be chosen to be $p = 20$ and for the fine grid at most $p = 4$, see Table 2. This implies that instead of 53 iterations for a coarse grid, 65 iterations are needed for a fine grid to solve the discretized problem. In other words, at the cost of 13 additional iterations we can use the fine grid while using the same amount of memory to store the Broyden matrix. The approximation of the cyclic steady state is qualitatively good using the coarse grid. However, the more accurate approximation using the fine grid is preferable, see Fig. 6.

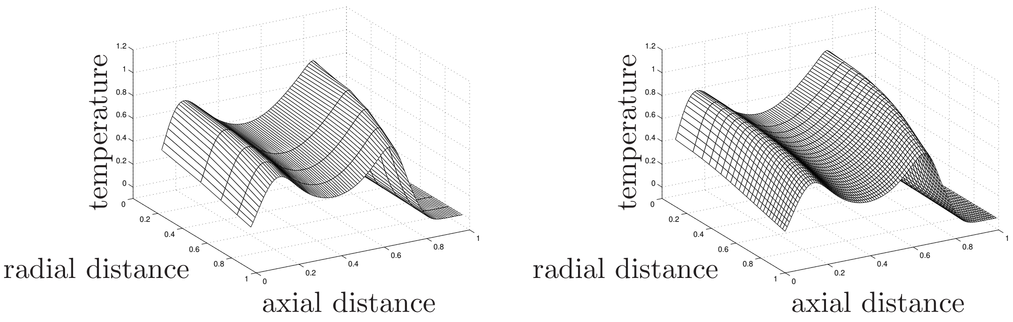

a) Coarse grid ($M = 5$) b) Fine grid ($M = 25$)

Fig. 6. Dimensionless temperature distribution over the reactor bed using a coarse and a fine grid ($R/L = 0.025$ and $\Phi = 0.2$).

4.2 Singular value distributions of the update matrices

For the Broyden Rank Reduction method the most important parameter is p, the maximum number of singular values of the update matrix that will be stored. As long as all singular values are stored, the process of the BRR(p) method is equal to the method of Broyden. The smaller the number p becomes, the more information of the update matrix is deleted. However, as we have seen, this does not necessarily imply slower convergence.

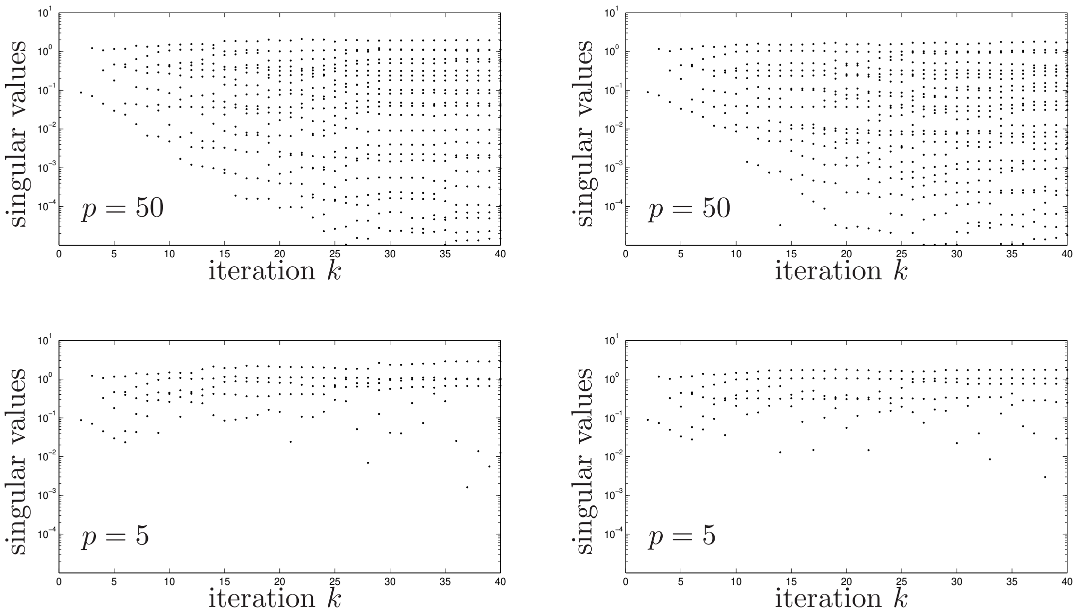

a) One-dimensional model b) Two-dimensional model

Fig. 7. The singular value distribution of the update matrix during the first 40 iterations of the BRR process, applied to the period map of the reverse flow reactor corresponding to the one-dimensional model and the two-dimensional model.

In Fig. 7 we have plotted the singular values of the update matrix during the first 40 iterations of the BRR process for $p = 5$ and $p = 50$, both for the one-dimensional model of Khinast *et al.* [5] and the two-dimensional model of Section 2. First we consider the results in Fig. 7(a) for the one-dimensional model. In case $p = 50$, we see that the update matrix has rank one at the start of the second iteration, that is, the matrix has one nonzero singular value. In every iteration one nonzero singular value is added. Note that, along the iterations the nonzero singular values are rather stable. Since for $k \leq p$ the BRR(p) iteration steps are plain Broyden steps, the singular value distributions corresponding to $p = 5$ and $p = 50$, respectively, are the same during the first 6 iterations. From the 7^{th} iteration, the singular value σ_5 starts oscillating. Observe from the two singular value distributions corresponding to the one-dimensional model, that the other four singular values are rather stable under the reduction procedure.

From Fig. 7(a) and Fig. 7(b), we observe that the singular value distributions produced by the BRR process for the one-dimensional and two-dimensional model are comparable. In agreement with the theory of Section 3 this implies, indeed, that the BRR method can be applied using the same value of p for both the one-dimensional and two-dimensional model.

5 Dynamic features of the two-dimensional model

In this section we will discuss the necessity of using a two-dimensional model in case of the existence of radial gradients. First, we show that radial gradients do exist, which can have the consequence that the one-dimensional and the two-dimensional model predict different conversion at the end of the reactor. Several Poincaré maps show that if the reactor width is sufficiently large, then the two-dimensional model predicts even different dynamical behavior compared to the one-dimensional model.

To obtain the results of this section dynamical simulation is used. Every simulation is started using a clean preheated bed, that is,

$$\theta = 1 \qquad \text{and} \qquad x = 1. \tag{18}$$

5.1 Existence and consequences of radial temperature gradients

We will show that radial temperature and conversion gradients can indeed occur if the radius of the reactor is sufficiently large. We describe the dynamical behavior of a thick reactor ($R/L = 0.025$) for a fixed value of the cooling capacity ($\Phi = 0.2$). The simulations are started with a clean preheated bed, see (18), and run for 50 iterations. We consider the state of the reactor at the end of the 50th flow reverse period.

Clearly, the cooling is especially influencing the temperature of the catalyst near the wall of the reactor. Moreover, we observe several differences between the one-dimensional and the two-dimensional model. For example, for different radial positions the axial position of the maximum temperature is shifted. In Fig. 8 also the conversion is given. Note that only around the axis the conversion is complete at the end of the reactor. Therefore the product gas consists of a mixture of both products and reactants. On average the prediction of the conversion is less than for the one-dimensional model.

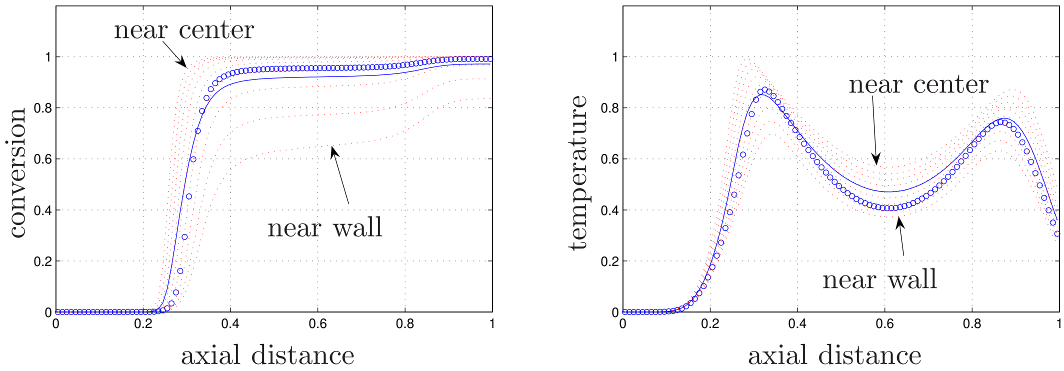

a) Conversion b) Temperature

Fig. 8. Dimensionless axial temperature and conversion profiles of the RFR before the 50th direction switch, in case of $\Phi = 0.2$ and $R/L = 0.025$. Dotted lines: profiles of the 2D-model at different radial distances; solid line: weighted average; circles: profile of 1D-model.

5.2 *Dependence of the qualitative dynamical behavior on radial temperature gradients*

We will now show that the radial temperature gradients can affect the long time dynamics of the reactor, by using Poincaré maps. For symmetric period-1 states, the Poincaré map consists of one single point and for asymmetric period-1 states, the Poincaré map has two points. In the figures of this section we show mainly the Poincaré map corresponding to quasi-periodic behavior. In this case the map consist of a set of points forming one or more closed curves. The Poincaré maps are constructed by considering $\Delta\theta_{\text{ave}}(n)$ versus $\theta_{\text{ave}}(n)$, where we define

$$\theta_{\text{ave}}(n) = \int_0^1 \bar{\theta}(z, nt_f)dz, \qquad n = 0, 1, 2, \ldots, \tag{19}$$

and

$$\Delta\theta_{\text{ave}}(n) = 2\Big(\int_0^{1/2} \bar{\theta}(z, nt_f)dz - \int_{1/2}^{1} \bar{\theta}(z, nt_f)dz\Big), \qquad n = 0, 1, 2, \dots . \quad (20)$$

Here $\bar{\theta}(z,t)$ is the average of the dimensionless temperature $\theta(z,r,t)$, see (7), over the cross section of the reactor at axial position z, that is,

$$\bar{\theta}(z,t) = 2\int_0^1 \theta(z,r,t)dr.$$

Hence the value $\theta_{\text{ave}}(n)$ is the average reactor temperature after the nth flow reversal and $\Delta\theta_{\text{ave}}(n)$ is the corresponding difference between the averaged temperatures in the right and left half of the reactor.

In Fig. 9 the Poincaré maps are given for $\Phi = 0.3$ and different values of the width of the reactor. In case of the one-dimensional model only one simulation is done since then the state of the reactor is independent of the width of the reactor. Every simulation consists of 2250 iterations and each iteration is represented by a dot. For the sake of presentation all even dots and odd dots are connected by a line. The transient phase started from the clean preheated bed, see (18), is a light line and the limiting phase (the last 1000 iterations) is a dark line.

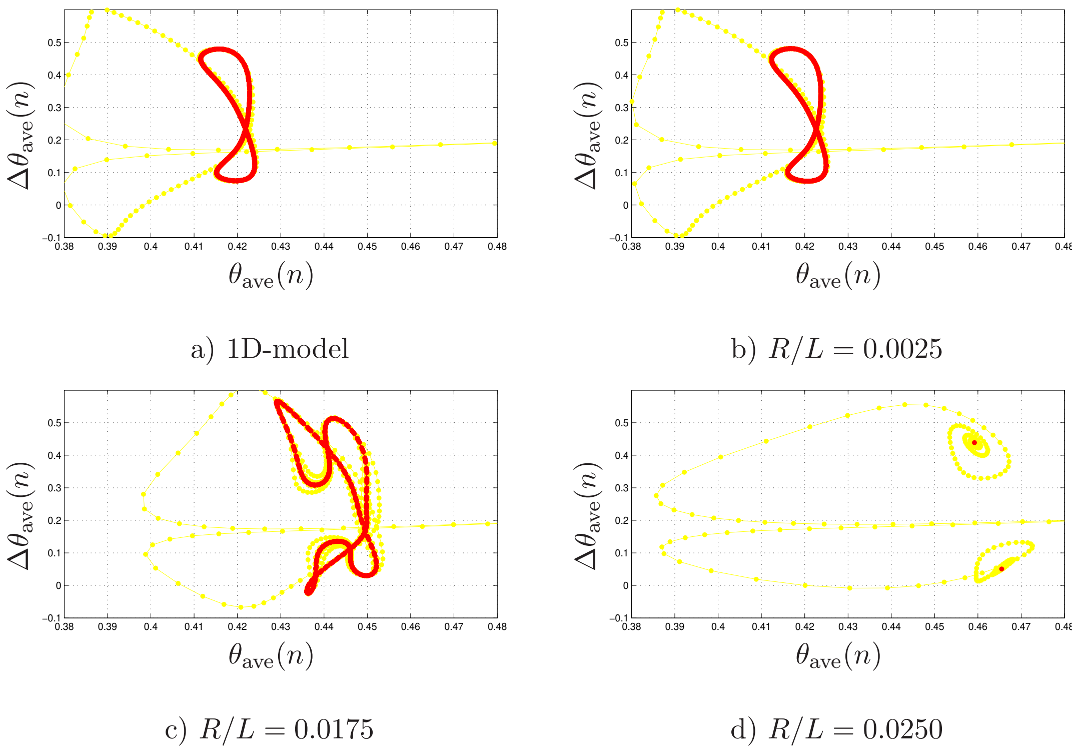

a) 1D-model

b) $R/L = 0.0025$

c) $R/L = 0.0175$

d) $R/L = 0.0250$

Fig. 9. Poincaré maps of the RFR for $\Phi = 0.3$ using the one-dimensional and the two-dimensional model for different values of R/L.

Several observations can be made from the Poincaré-maps given in Fig. 9. For a thin reactor ($R/L = 0.0025$) the one-dimensional model and the two-dimensional model give the same results. However we see that the long time dynamics depend strongly on the width of the reactor. For $R/L = 0.025$ the separated curves converge to singles points, which implies that the quasi-periodic behavior changes into asymmetric periodic behavior. For more details of these computations we refer to [13]

6 Conclusions

We have introduced a new method, called the Broyden Rank Reduction (p) method, to efficiently compute long time dynamics of periodically forced processes. This allows us for the first time to simulate a full two-dimensional model, where radial gradients cannot be neglected. The principle of the Broyden Rank Reduction method is practically applicable because n-dimensional computations, concerning the inverse of the Broyden matrix and the singular value decomposition of the update matrix, are reduced to computations in the p-dimensional space, where $p \ll n$. The simulations in Example 2 and for the reverse flow reactor show that p depends on properties of the period map of the dynamical system rather than the number of grid points in the mess of the discretization. This fact is very useful in practical applications. We can start a simulation on a coarse grid where memory constraints are no issue, and a suitable value of p can easily be found. Next we redo the simulations on a fine grid, using the earlier found value of p. This reduces the amount of memory needed for the simulations and allow accurate computations that were not possible before.

The code of the BRR(p) and other limited memory Broyden methods is available in [11].

References

[1] C.G. Broyden, A class of methods for solving nonlinear simultaneous equations, *Math. Comp.* **19** (1965) 577–593.

[2] D.T. Croft and M.D. Levan, Periodic states of adsorption cycles–i: direct determination and stability, *Chem. Eng. Sci.* **49** (1994) 1821–1829.

[3] J.E. Dennis, Jr. and R.B. Schnabel, *Numerical methods for unconstrained optimization and nonlinear equations*, volume **16** of *Classics in Applied Mathematics*, Soc. for Ind. and Appl. Math. (SIAM), Philadelphia, PA, 1996. Corrected reprint of the 1983 original.

[4] N. Gould, D. Orban, and Ph.L. Toint, Numerical methods for large-scale nonlinear optimization, *Acta Numer.* **14** (2005) 299–361.

[5] J.G. Khinast, Y.O. Jeong, and D. Luss, Dependence of cooled reverse-flow reactor dynamics on reactor model, *AIChE J.* **45** (1999) 299–309.

[6] J. Sánchez, M. Net, B. García-Archilla, and C. Simó, Newton-Krylov continuation of periodic orbits for Navier-Stokes flows, *J. Comput. Phys.* **201** (2004) 13–33.

[7] L.K. Schubert, Modification of a quasi-Newton method for nonlinear equations with a sparse Jacobian, *Math. Comp.* **24** (1970) 27–30.

[8] O.J. Smith and A.W. Westerberg, Acceleration of cyclic steady state convergence for pressure swing adsorption models, *Ind. Eng. Chem. Res.* **31** (1992) 1569–1573.

[9] G. Strang, *Introduction to Linear Algebra*, Wellesley-Cambridge Press, 1998.

[10] Ph.L. Toint, Numerical solution of large sets of algebraic nonlinear equations, *Math. Comp.* **46** (1986) 175–189.

[11] B.A. van de Rotten, *A limited memory Broyden method to solve high-dimensional systems of nonlinear equations*, PhD thesis, Universiteit Leiden, 2003. http://www.math.leidenuniv.nl/docs/.

[12] B.A. van de Rotten and S.M. Verduyn Lunel, A limited memory Broyden method to solve high-dimensional systems of nonlinear equations, *submitted*.

[13] B.A. van de Rotten, S.M. Verduyn Lunel, and A. Bliek, Efficient simulation of periodically forced reactors with radial gradients, *Chemical Engineering Science* **61** (2006) 6981–6994.

[14] T.L. van Noorden, S.M. Verduyn Lunel, and A. Bliek, Acceleration of the determination of periodic states of cyclically operated reactors and separators, *Chem. Eng. Sci.* **57** (2002) 1041–1055.

[15] T.L. van Noorden, S.M. Verduyn Lunel, and A. Bliek, Optimization of cyclically operated reactors and separators, *Chem. Eng. Sci.* **58** (2003) 4115–4127.

[16] K.R. Westerterp, W.P.M. van Swaaij, and A.A.C.M. Beenackers, *Chemical Reactor Design and Operation*, John Wiley & Sons Ltd., second edition, 1988.